

Supporting Information

Enhanced Ion Transport by Graphene Oxide /Cellulose Nanofibers

Assembled Membranes for High-performance Osmotic Energy Harvesting

Yadong Wu,^{a,b} Weiwen Xin,^{a,b} Xiang-Yu Kong,^b Jianjun Chen,^b Yongchao Qian,^b Yue Sun,^b

Xiaolu Zhao,^b Weipeng Chen,^b Lei Jiang,^b Liping Wen^{*,a,b}

^a CAS Key Laboratory of Bio-inspired Materials and Interfacial Science, Technical Institute of Physics and Chemistry, Chinese Academy of Sciences, Beijing 100190, P. R. China.

^b School of Future Technology, University of Chinese Academy of Sciences, Beijing 100049, P. R. China.

* wen@mail.ipc.ac.cn

Table of contents

1. Materials
2. Fabrication of GO/CNFs membrane
3. Electrical measurements
4. Characterization
5. Electrode calibration
6. Energy conversion efficiency
7. Membrane preparation and structure characterization
8. Pure GO membrane structure characterization
9. The basic equivalent circuit
10. The influences of the electrolyte species on output energy density
11. The influence of the thickness on output energy density

12. The influence of the valent of mobile ions on output energy density
13. The immersing-dependence relationship for energy conversion performance
14. The XRD spectrum for hydrated and ambient dried membranes
15. Thermal-dependence relationship for GO/CNFs energy conversion performance
16. The energy barrier for Na⁺ ion permeation of GO membrane
17. Comparison of the power output for GO/PVA and GO/CNFs membranes
18. Zeta electric potential
19. Stability test

1. Materials

Graphene oxide (thickness 0.8-1.2 nm, diameter 0.5-5 μm) was purchased from J&K Beijing Co., Ltd. TEMPO-oxidized CNFs gel (1 wt%, hemicellulose ~15%) was purchased from Tianjin Woodelfbio Cellulose Co., Ltd. PVA ($M_w \sim 100,000$) were purchased from Sigma. All the chemicals including HCl, KOH, sodium chloride (NaCl), potassium chloride (KCl), and lithium chloride (LiCl) were analytically pure. Deionized water with a resistivity of 18.25 $M\Omega\text{ cm}$ was used in all experiments.

2. Fabrication of GO/CNFs Membrane

The CNFs (0.8~2.0 μm in length and 1~10 nm in diameter) were dispersed in deionized water, then sonicated for 20 min to yield a CNFs suspension at 1mg/mL. GO was dispersed and sonicated in deionized water to get a uniform suspension at 1 mg/mL under the similar process described above all. GO/CNFs assembled suspension was obtained by a simple mixed certain amount (10 mL) of CNFs and (5 mL) GO suspension. Then it was sonicated for 20 min to form a uniform suspension. The final GO/CNFs mixture was filtered through PC filter (47 mm in diameter, 0.44 μm nominal pore size) and followed by drying in the air for 12h, the GO/CNFs assembled membrane could be easily peeled from the PC substrate. The corresponding comparison pure GO, CNFs and GO/PVA membranes were obtained through a similar process.

3. Electrical measurements

The electrochemistry measurements including I-V and osmotic energy conversion tests were performed with a Keithley 6487 semiconductor picoammeter (Keithley Instruments, Cleveland, OH). The measurement equipment consisted of two-compartment conductivity cells which sandwiched tested membrane and a pair of homemade Ag/AgCl electrodes providing a transmembrane potential. The membrane was replaced by a nonselective silicon membrane containing a single micro-window to obtain the experimental value of V_{redox} (Table S1). The effective membrane area is $3 \times 10^4 \mu\text{m}^2$. The electrolyte was adjusted to the desired pH using NaOH or HCl for different pH test.

4. Characterization

The SEM image was captured using scanning electron microscopy (HITACHI S-4800). The AFM image was captured using Atomic force microscopy (Bruker Multimode 8). The X-ray

diffraction (XRD) analysis was carried out by using the Bruker D8 focus. Before fully hydrated XRD test, the membrane was immersed in a 0.5 M NaCl solution for least 24 hours at ambient temperature to be fully hydrated. Then the fully hydrated membrane was quickly taken out of solution and followed by the XRD test. The Zeta potential test was performed in a solution system using a Zetasizer (NanoZSP, Malvern Instruments Ltd., Malvern, UK).

5. Electrode calibration

The I-V curves were used to explore the osmotic energy harvesting performance under the experimental setup illustrated in Figure S3. Specifically, the sweeping voltage range from -200 mV to 200 mV by a uniform step (20 mV). V_{diff} , V_{redox} and V_{oc} mean diffusion potential contributed by the ion selective membrane, unequal potential drop induces redox potential and the measured potential respectively. $R_{channel}$ represents membrane resistance and $R_{resistance}$ means electronic load resistance. The sum of V_{diff} and V_{redox} is equal to V_{oc} , thus to obtain V_{diff} , V_{redox} needs to be excluded. Here, an experimental method¹⁻³ is applied to get V_{redox} where records the potential under a certain osmotic gradient without membrane, the measured voltage was determined individually by the V_{redox} .

6. Energy conversion efficiency

Under an osmotic gradient, the cation transference number (i.e. t^+) and energy conversion efficiency can be calculated according to the following equation.

$$V_{diff} = (t_+ - t_-) \frac{RT}{F} \ln\left(\frac{a_{high}}{a_{low}}\right) = (2t_+ - 1) \frac{RT}{F} \ln\left(\frac{a_{high}}{a_{low}}\right)$$

$$\eta_{max} = \frac{1}{2} (2t_+ - 1)^2$$

Here t^+ and t^- are the transference numbers for positively and negatively charged ions, respectively. R , T , F are the universal gas constant, the absolute temperature, and the Faraday constant, respectively. The a_{high} and a_{low} represent the activities of electrolyte in the high concentration and low concentration side respectively. Accordingly, the energy conversion efficiency corresponding to the maximum power generation can be calculated through the method described above all.

7. Membrane preparation and structure characterization.

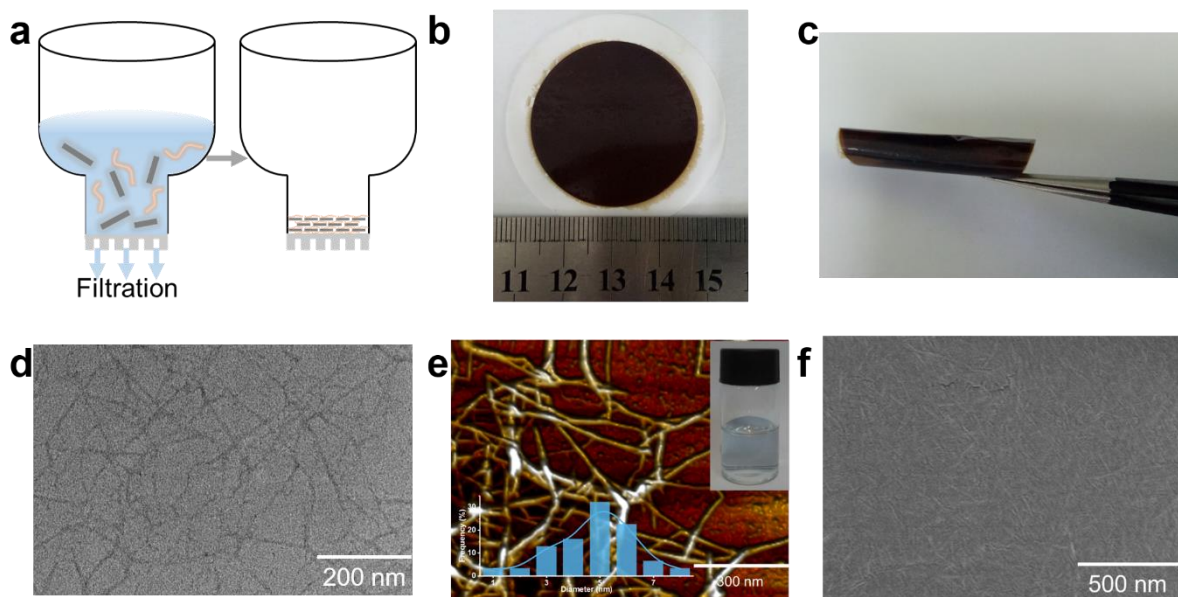


Figure S1. (a) Vacuum-assisted filtration process to prepare the GO/CNFs membrane. (b, c) A photograph of the GO/CNFs membrane, showing the homogeneity and the flexibility in large surface scale membrane. (d, e) AFM and TEM images of CNFs with length in micrometer scale and diameter in the range of 1-10 nm (average diameter ~ 4.80 nm). (f) SEM image of GO/CNFs shows the existence of CNFs on the surface of the GO/CNFs membrane.

8. Pure GO membrane structure characterization.

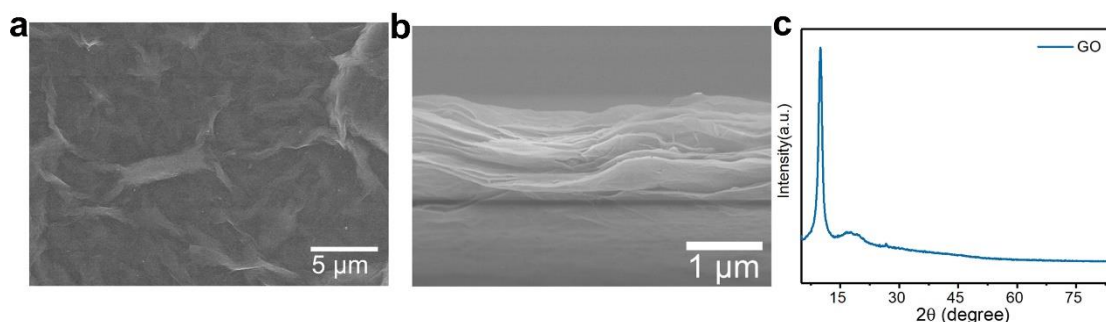


Figure S2. (a) SEM for pure GO membrane which has not any fiber-like structure on the surface. (b) Cross-sectional SEM image of lamellar structured GO membrane which shows the clear layered structure. (c) XRD patterns of pure GO membrane indicates a narrow interlayer distance of 0.88nm.

9. The basic equivalent circuit.

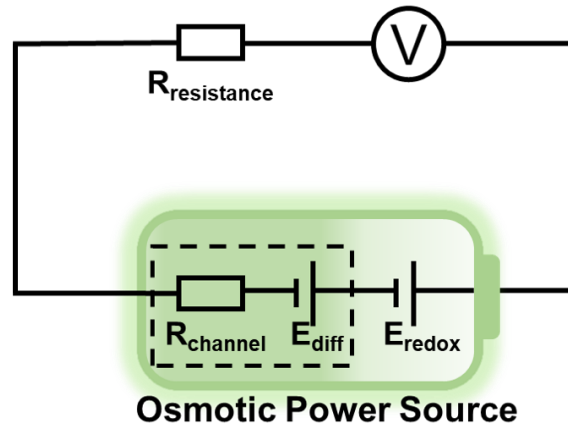


Figure S3. The equivalent circuit for the membrane-based osmotic power source.

10. The influence of the membrane types and electrolyte species on output energy density.

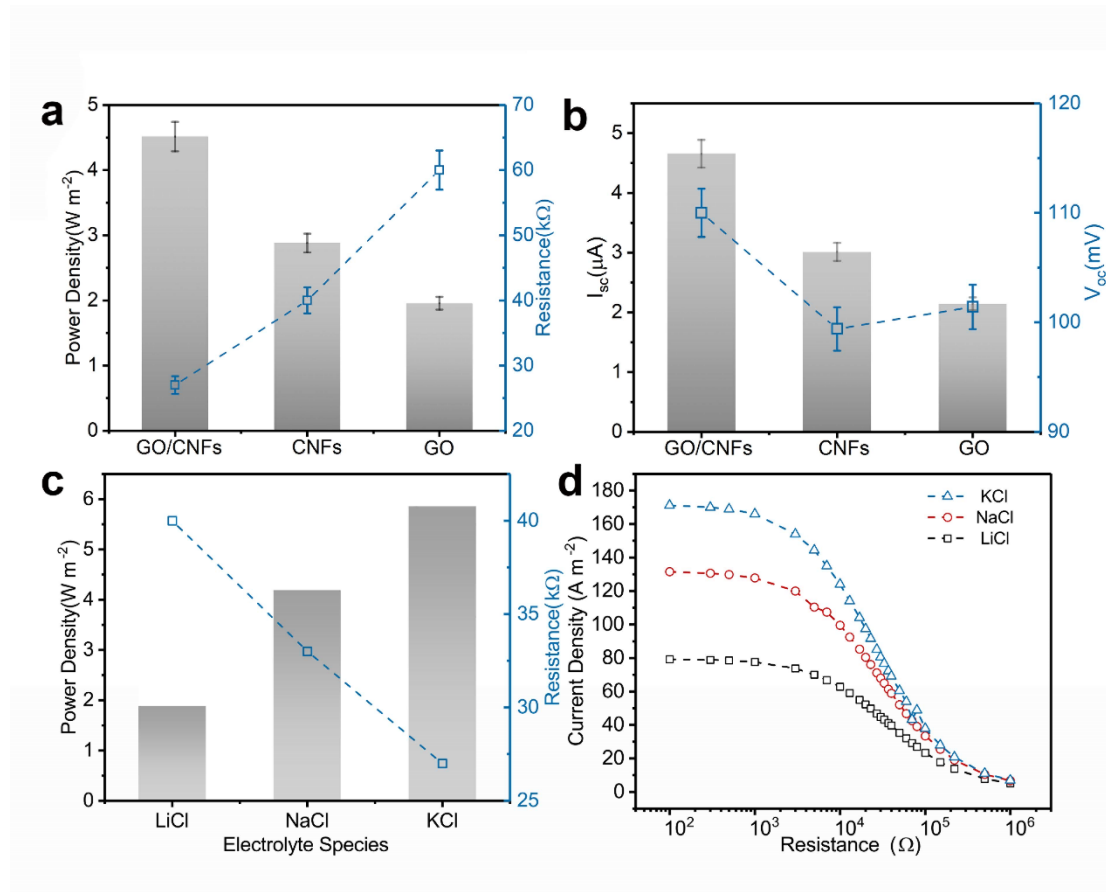


Figure S4. (a) The output power density and resistance comparison for GO/CNFs versus pure CNFs and pure GO membrane, representing an improved power density and reduced resistance. (b) The short-circuit (I_{sc}) and open-circuit voltage (V_{oc}) comparison for GO/CNFs versus pure CNFs and pure GO membrane, showing an increment for both flux and selectivity attributing to the function of space charge. (c) The dependence of the electrolyte species on the output power density. Error bars represent s.d. (d) The dependence of the electrolyte species on the

current density over a range of load resistance.

11. The influence of the thickness on output energy density.

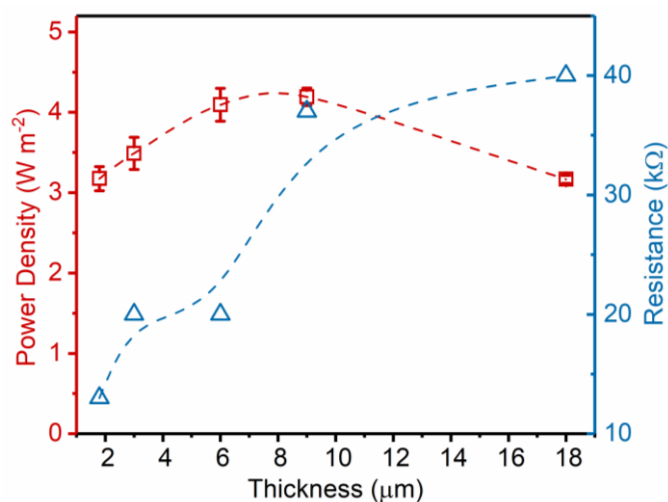


Figure S5. Influence of the thickness on the power density and resistance

12. The influence of the valent of mobile ions on output energy density.

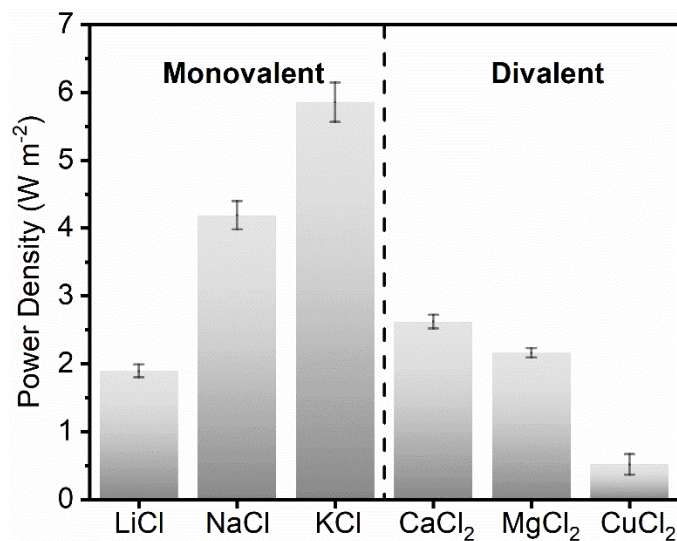


Figure S6. Influence of the valent of the mobile ions on the power density. The osmotic power is lower for divalent (Ca^{2+} , Mg^{2+} , Cu^{2+}) cations compared with that of the monovalent (Li^+ , Na^+ , K^+) cations because of bigger hydrated diameter and lower ion diffusion coefficients.

13. The immersing-dependence relationship for energy conversion performance.

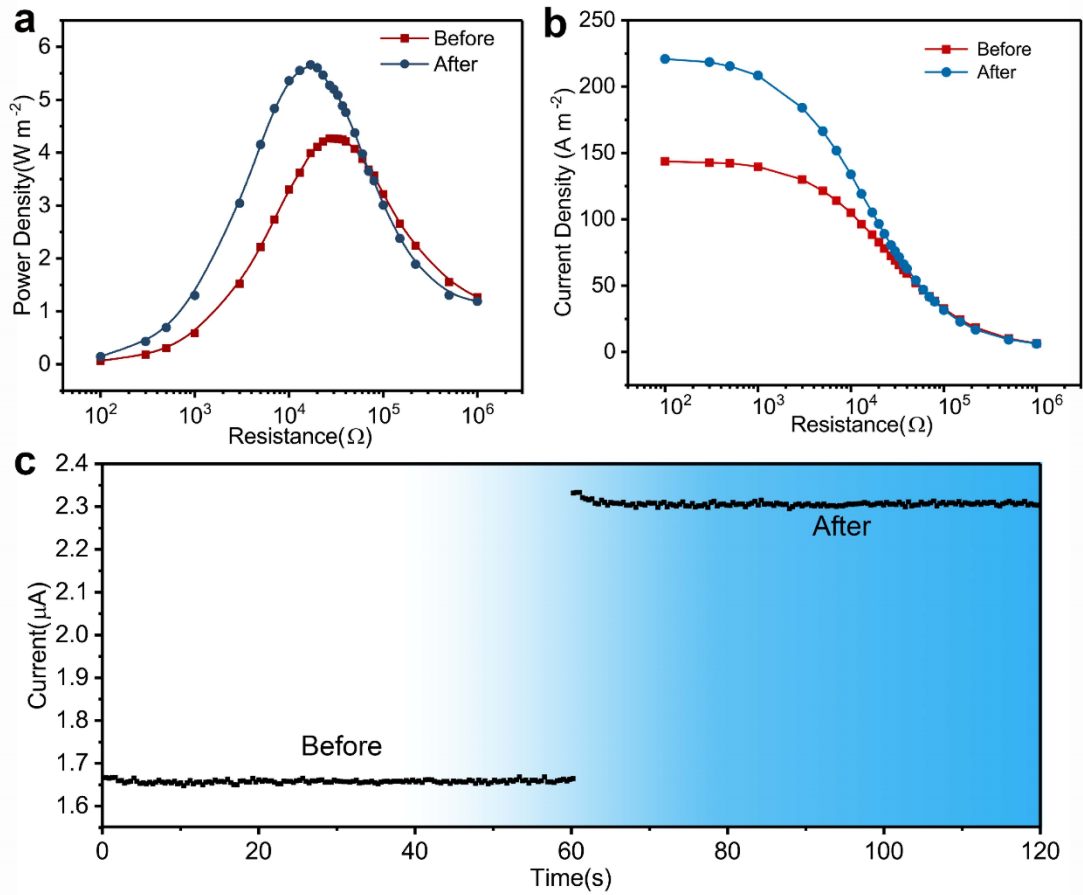


Figure S7. (a) The immersing-dependence relationship for GO/CNFs energy conversion performance. (b) The corresponding current density comparison for GO/CNFs membrane before and after immersing. (c) The current comparison at the largest power density output for GO/CNFs membrane before and after immersing, which represents improved and stable output current density over time, thus the membrane has been activated.

14. The XRD spectrum for hydrated and ambient dried membranes

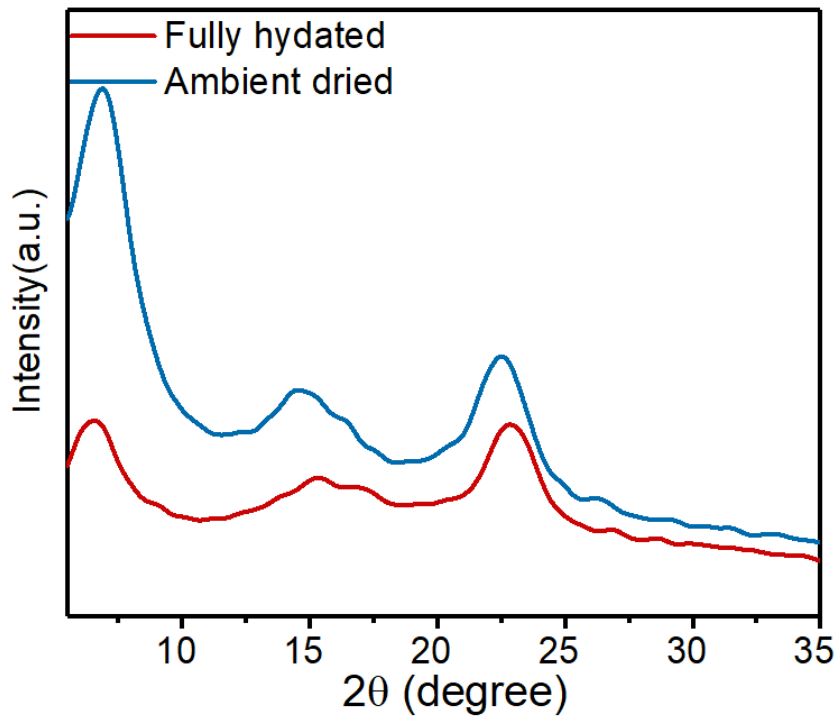


Figure S8. The XRD spectrum for fully hydrated and ambient dried membrane, confirming the chemical stability and enlarged interlayer distance.

15. Thermal-dependence relationship for GO/CNFs energy conversion performance.

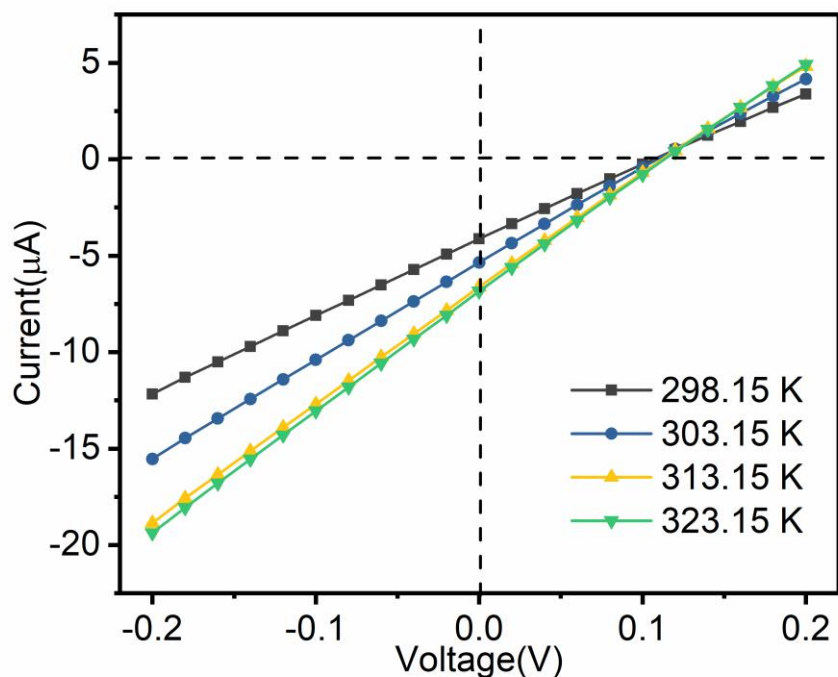


Figure S9. The representative I - V characteristics at different temperatures.

16. The energy barrier for Na^+ ion permeation of GO membrane.

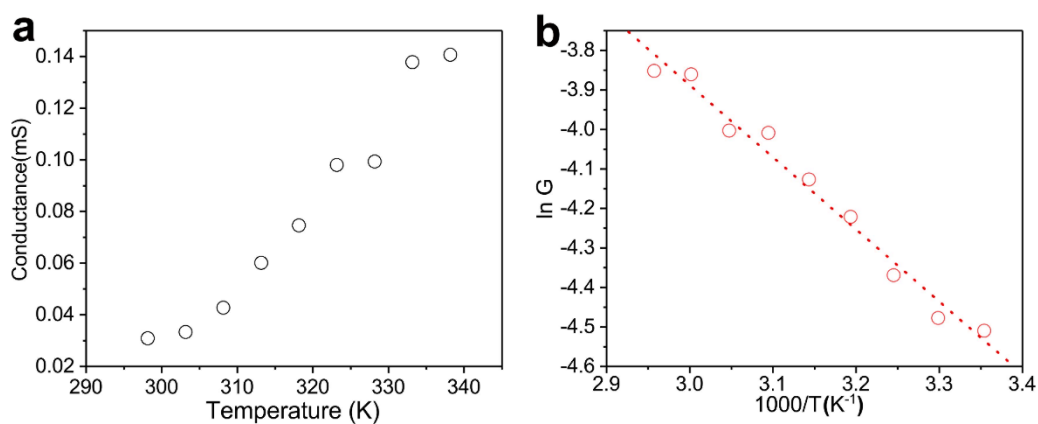


Figure S10. (a) Ionic conductance at different temperatures in 10 mM NaCl. (b) The Arrhenius plot of the conductance, $\ln(G)$ versus inverse temperature ($1000/T$). The calculated energy barrier for Na^+ ion permeation is revealed to be 15.18 kJ/mol comparable to the reported value with similar interlayer distance⁴⁻⁶.

17. Comparison of the power output for GO/PVA and GO/CNFs membranes.

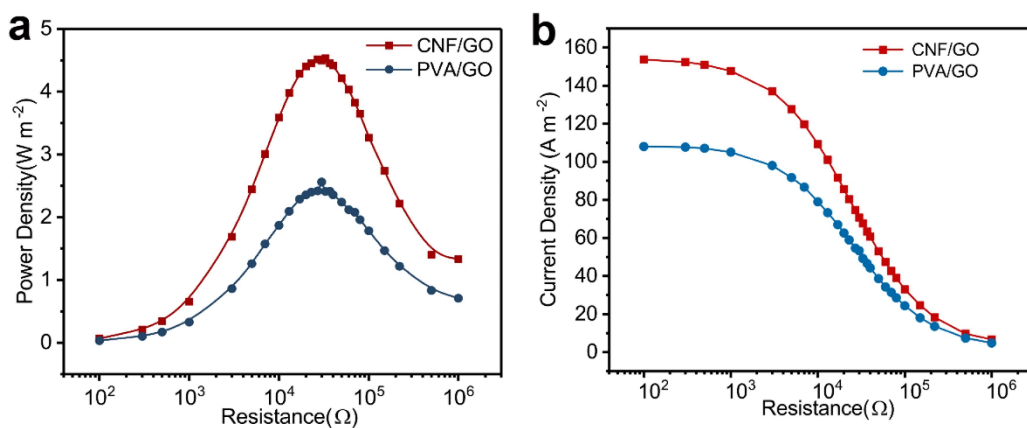


Figure S11. (a) Comparison for the power output of high space charge GO/CNFs and less space charge GO/PVA membranes with the same weight ratio, which illustrates the important role of space charge for energy conversion. (b) A comparison for the current density of GO/CNFs and GO/PVA membranes showing the improved current density by higher space charge.

18. Zeta electric potential.

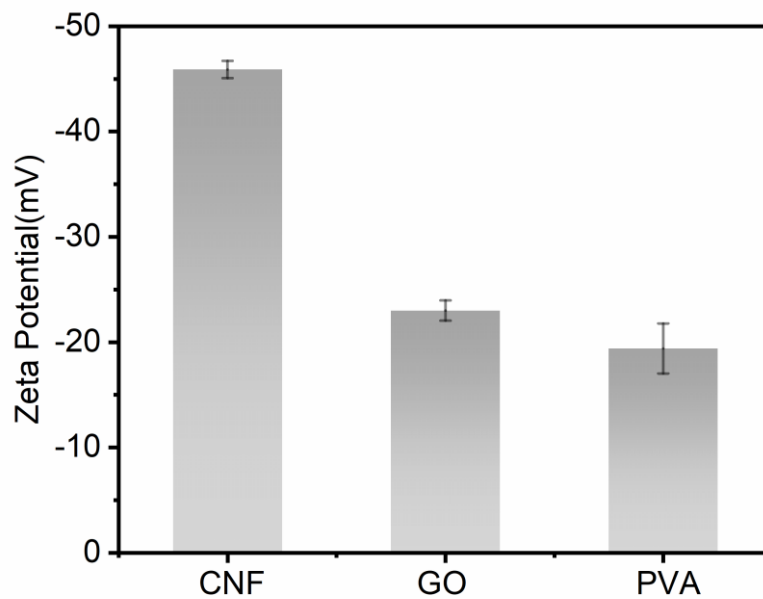


Figure S12. Zeta potential comparison for CNFs, GO and PVA.

19. Stability test.

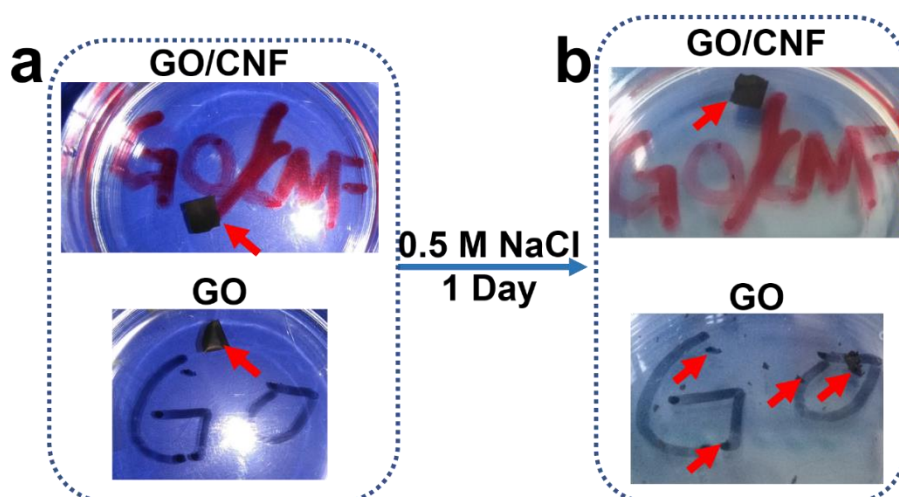


Figure S13. Stability test for GO/CNFs and GO membranes. (a) Just immersing membranes in 0.5 M NaCl. (b) After immersing membranes in 0.5 M NaCl for 24 hours and testing the output power density which illustrates CNFs increased the stability of membrane at the same time comparing with the pure GO membrane.

Table S1. List of V_{oc} , V_{redox} and V_{diff} under different concentration gradients.

| Concentration Gradient (C_H/C_L) | $10^{-5}/10^{-4}$ | $10^{-5}/10^{-3}$ | $10^{-5}/10^{-2}$ | $10^{-5}/10^{-1}$ | $10^{-5}/1$ | $10^{-5}/2$ | $10^{-5}/3$ |
|--------------------------------------|-------------------|-------------------|-------------------|-------------------|-------------|-------------|-------------|
| V_{oc} | 27 | 86 | 159 | 226 | 270 | 276 | 285 |
| V_{redox} | 19 | 45 | 72 | 81 | 93 | 97 | 105 |
| V_{diff} (mV) | 8 | 41 | 87 | 145 | 177 | 179 | 180 |

Supplementary References

- 1 C. Wang, C. Miao, X. Zhu, X. Feng, C. Hu, D. Wei, Y. Zhu, C. Kan, D. Shi and S. Chen, *ACS Appl. Nano Mater.*, 2019, **2**, 4193–4202.
- 2 J.-J. Shao, K. Raidongia, A. R. Koltonow and J. Huang, *Nat. Commun.*, 2015, **6**, 7602.
- 3 J. Abraham, K. S. Vasu, C. D. Williams, K. Gopinadhan, Y. Su, C. T. Cherian, J. Dix, E. Prestat, S. J. Haigh, I. V. Grigorieva, P. Carbone, A. K. Geim and R. R. Nair, *Nat. Nanotechnol.*, 2017, **12**, 546–550.
- 4 Z. Zhang, S. Yang, P. Zhang, J. Zhang, G. Chen and X. Feng, *Nat. Commun.*, 2019, **10**, 2920.
- 5 W. Xin, Z. Zhang, X. Huang, Y. Hu, T. Zhou, C. Zhu, X.-Y. Kong, L. Jiang and L. Wen,

Nat. Commun., 2019, **10**, 3876.

- 6 Z. Zhang, X. Sui, P. Li, G. Xie, X.-Y. Kong, K. Xiao, L. Gao, L. Wen and L. Jiang, *J. Am. Chem. Soc.*, 2017, **139**, 8905–8914.